



HAL
open science

Structure-activity relationship and molecular modelling studies of quinazolinedione derivatives MMV665916 as potential antimalarial agent

Laura Mourot, Marjorie Schmitt, Elisabeth Mouray, Martin Spichty, Isabelle Florent, Sébastien Albrecht

► **To cite this version:**

Laura Mourot, Marjorie Schmitt, Elisabeth Mouray, Martin Spichty, Isabelle Florent, et al.. Structure-activity relationship and molecular modelling studies of quinazolinedione derivatives MMV665916 as potential antimalarial agent. *Bioorganic and Medicinal Chemistry Letters*, 2021, 51, pp.116513. 10.1016/j.bmc.2021.116513 . hal-03432154

HAL Id: hal-03432154

<https://hal.science/hal-03432154v1>

Submitted on 17 Nov 2021

HAL is a multi-disciplinary open access archive for the deposit and dissemination of scientific research documents, whether they are published or not. The documents may come from teaching and research institutions in France or abroad, or from public or private research centers.

L'archive ouverte pluridisciplinaire **HAL**, est destinée au dépôt et à la diffusion de documents scientifiques de niveau recherche, publiés ou non, émanant des établissements d'enseignement et de recherche français ou étrangers, des laboratoires publics ou privés.

Structure-Activity relationship and molecular modelling studies of quinazolinone derivatives MMV665916 as potential antimalarial agent.

Laura Mourot^a, Marjorie Schmitt^a, Elisabeth Mouray^b, Martin Spichy^a, Isabelle Florent^b, Sébastien Albrecht^{a*}

a Université de Haute-Alsace, Université de Strasbourg, CNRS, LIMA UMR 7042, F-68000 Mulhouse, France.

b Unité Molécules de Communication et Adaptation des Micro-organismes, UMR7245, Muséum National d'Histoire Naturelle, CNRS, Sorbonne Universités, Paris, France.

* corresponding author

Email address : sebastien.albrecht@uha.fr

Abstract

A series of new quinazolinone derivatives have been readily synthesized and evaluated for their *in vitro* antimalarial growth inhibition activity. Most of the compounds inhibited *P. falciparum* FcB1 strain in the low to medium micromolar concentration. Compounds **7g**, **7i** and **7k** showed the best inhibitory activity with EC₅₀ values around 5 μM. However, these compounds were less potent than the original hit MMV665916, which showed remarkable growth inhibition with EC₅₀ value of 0.4 μM. In addition, a novel approach for determining the docking poses of these quinazolinone derivatives with their potential protein target, the *P. falciparum* farnesyltransferase PfFT, was investigated.

Keywords

antiplasmodial activity, quinazolinone series, molecular docking, farnesyltransferase

1. Introduction

With an estimated 229 million cases and 409 000 related deaths in 2019,¹ malaria is still one of the most severe public health problems worldwide. In the two recent decades, malaria prevention and control strategies in endemic areas have allowed a net decrease in morbidity and mortality. However, many challenges, including drug and insecticide resistance, threaten the malaria control efforts. Indeed, decreased efficacy of artemisinin derivatives and new resistance to partner drugs in artemisinin combination therapies (ACTs), the frontline treatments for uncomplicated *falciparum* malaria, have led to the rising of treatment failures or delayed parasite clearance.¹⁻³ The discovery of novel *Plasmodium* molecular targets or original antimalarial agents with new mode of action are thus urgently needed to combat malaria. According to WHO's recommendation, useful antimalarial drugs must possess activity against multiple stages of the parasite's life cycle, be rapidly acting and highly efficacious. Highly desirable drugs should target in priority dormant malaria parasites from the liver and block the transmission of *Plasmodium*.⁴⁻⁶

We focused our attention on the Medicine for Malaria Venture "Malaria Box", a collection of 400 drug-like or probe-like compounds with activity against *P. falciparum* blood stage and having no significant toxicity to humans, which was made available to the international community to foster the antimalarial drug discovery.⁷ We were interested in identifying compounds displaying activity against the erythrocytic and hepatic stages of *Plasmodium*. We also took into consideration their synthetic tractability. Indeed, synthetic ease and cost-of-goods should be relatively low to provide a medicine affordable for everyone. After data mining and visual inspection of the "Malaria Box", we have identified the quinazolidione-based scaffolds, MMV665916 and MMV019066, that demonstrated interesting biological properties against multiple life cycle stages of the malaria parasite. They displayed potent parasite growth inhibitory activities ($< 1 \mu\text{M}$ against different *P. falciparum* strains, including parasite lines with resistance to known antimalarials). They were active *on* liver stage (*P. berghei*-Luc $\text{IC}_{50} < 0.1 \mu\text{M}$)^{8,9} by inhibiting parasite replication during exoerythrocytic-parasite stages development.⁸ These quinazolidione-based compounds showed a remarkable selectivity window with a low toxicity for human cells (MRC5 fibroblasts $\text{EC}_{50} > 32 \mu\text{M}$) and no cardiotoxicity risk (hERG inhibition).⁹

However, pharmacokinetic issues were encountered for both quinazolidione derivatives, and included poor overall exposure (AUC) and/or low to modest plasma C_{max} . Key *in vitro* ADME properties might require improvements, such as protein binding and aqueous solubility, that could be a limiting factor for oral absorption, whereas a high liver metabolism might account for the poor exposure upon oral administration.¹⁰

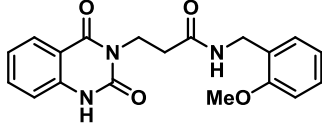
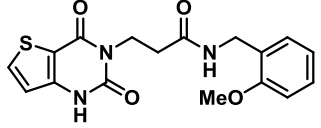
		 MMV665916	 MMV019066
Antiplasmodial activity	Asexual blood stage ⁹ <i>P. falciparum</i> strains (3D7, K1, W2, Dd2, FCR3) EC ₅₀	Active (0.07 to 0.54 μM)	Active (0.07 to 0.98 μM)
	Sexual stage ¹¹⁻¹⁵ <i>P. falciparum</i> early and late gametocytes	Inactive	Inactive
	Liver stage ^{8,9} <i>P. berghei</i> % of control infection @ 5 μM	Active (23%)	Active (27%)
	<i>P. berghei</i> -Luc IC ₅₀	44 nM	56 nM
	Ookinete ¹⁶ <i>P. berghei</i> ookinete development IC ₅₀	Inactive	Inactive
Toxicity ⁹	MRC-5 EC ₅₀	> 32 μM	> 32 μM
	hERG liability (inhibition % @ 11 μM)	No (19%)	No (5%)
In vitro ADME ⁹	Kinetic solubility (>20 μM @ pH 7.4)	No	Yes
	Human PPB (fraction bound)	>95%	< 95%
PK ⁹ (Mouse oral single dose 140 μmol/kg)	C_{max} (> 1 μM)	No (0.0213)	Yes
	T_{max} (h)	0.25	-
	AUC₀₋₇ (> 12 h.μM)	No (0.0729)	No
	MRT₀₋₇ (h)	3.01	-

Table 1. PK data were kindly given, personal communication with MMV.

We then carried out a structural optimization of the MMV665916 compound to improve its potency and address some of its *in vitro* and *in vivo* ADME liabilities, with a focus on improving metabolic stability. The structural modifications were focused on three regions: the N-benzylamide part (region A), the linker (region B) and the quinazolinone core (region C).

Rapid exploration of structure-activity relationships (SAR) was made possible due to the expedient synthesis and readily preparation of a variety of analogues. A total of twenty-seven compounds were synthesized and the structure-activity relationship against erythrocytic stages of the *P. falciparum* FcB1 strain in culture was further explored.

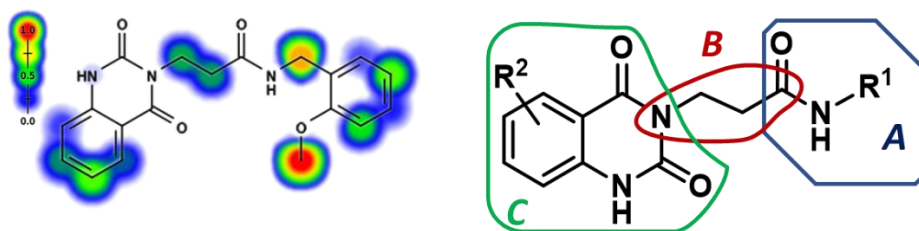
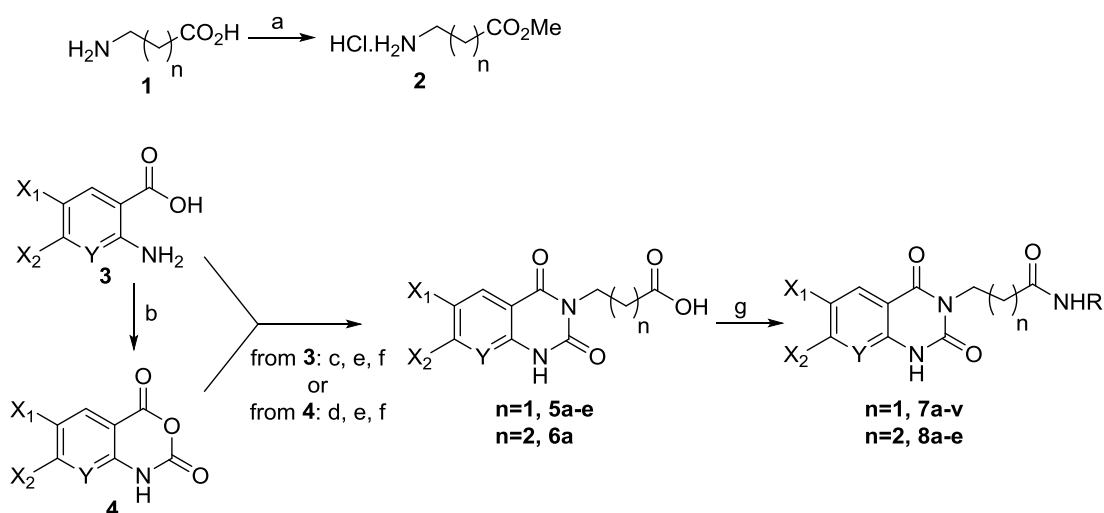


Figure 1. a) Xenosite Cytochrome P450 metabolism site prediction for MMV665916.^{17–19} The blue to red gradient color scale represents the likelihood of metabolic degradation. Site of metabolism highlighted in red being the most likely metabolic hotspot. b) Planned optimization studies of the quinazolinone-based antimalarial compound.

2. Results and Discussion

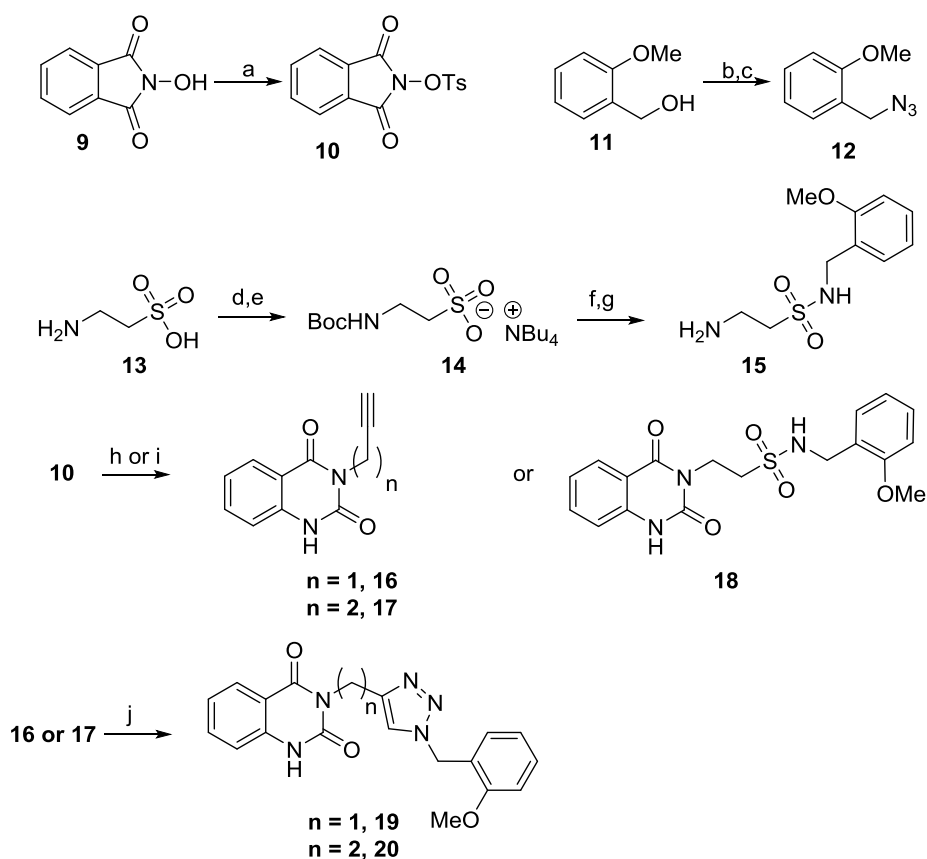
2.1 Chemistry

The different 3-substituted quinazoline-2,4-diones **5** and **6** were obtained by two different routes. An amino acid methyl ester hydrochloride salt **2**, derived from β -alanine or γ -aminobutyric acid, readily synthesized from the corresponding amino acid **1** with thionyl chloride in MeOH, was coupled with anthranilic acid **3** in presence of HBTU in DMF. A second route involved the reaction of compound **2** with isatoic anhydride electrophile **4** in THF in the presence of DIPEA at 70°C. When the isatoic anhydride was not commercially available, it was readily accessible by cyclocondensation between the corresponding anthranilic acid and solid triphosgene in a mixture of MeCN/DCM. Next, the resulting *N*-alkyl-*o*-aminobenzamide intermediates were converted into the required *N*-alkylated quinazolinone derivatives **5** and **6** by a sequential intermolecular aniline coupling with ethylchloroformate, followed by cyclization of the resulting carbamate upon treatment with NaOH at 70°C. Concomitantly, the ester function was saponified upon alkaline treatment. The resulting carboxylic acids were coupled with various aliphatic or aromatic amines to give the title compounds **7a-v** and **8a-e**. Among various peptide coupling agents screened, the system HBTU/DIPEA in DMF was the best condition for non-challenging amide bond formation. However, as soon as the amine counterpart was sterically hindered or poorly nucleophile, the COMU/DIPEA in DMF condition was the most efficient reagent combination to perform peptide coupling reaction. Finally, replacement of DMF by dioxane allowed the precipitation of the desired products which were easily purified by a simple filtration and wash procedure.



Scheme 1. Synthesis of. Reagents and conditions: a) SOCl_2 , MeOH, 0°C to 70°C , 5h. b) Triphosgene, pyridine, MeCN : CH_2Cl_2 (4/1), 55°C , 24h. c) **2**, HBTU, DIPEA, DMF, RT, 72h. d) **2**, DIPEA, THF, 70°C , 18h. e) Ethylchloroformate, K_2CO_3 , CH_2Cl_2 , RT, 24h. f) NaOH, EtOH, 70°C , 20-48h. g) R-NH₂, DIPEA, HBTU or COMU, DMF or dioxane, RT or 50°C , 48-72h.

Peptide bond isosteres. Next, we turned our attention to the synthesis of peptide bond isosteres, like sulfonamide and triazole motifs.^{20,21} The sulfonamide analogue **18** and the triazole derivatives **19** and **20** were readily prepared according to scheme 2. Their synthesis commenced with the preparation of azido precursors **12** and with the β -aminosulfonamide derivative **15**, obtained in 4 steps from taurine.²² The key reaction involved the formation of the quinazolinone core, which was performed via a Lossen rearrangement and subsequent ring closure of N-tosyloxypthalimide **10** in presence of various amine nucleophile,²³ leading to the linear alkyne precursors **16** and **17** and to the sulfonamide analogue **18**. Next, the Cu(II)/ascorbate-catalyzed click chemistry²⁴ provided rapid access to the two additional 1,4-disubstituted 1,2,3-triazole analogues **19** and **20**.



Scheme 2. Synthesis of amide bond isosteres **18–20**. Reagents and conditions: a) TsCl, pyridine, CH₂Cl₂, RT, 77%. b) MsCl, Et₃N, CH₂Cl₂, 0°C. c) NaN₃, MeCN, 85°C, 24h, 62% (2 steps). d) Boc₂O, NaOH, THF, RT, 15h. e) LiOH.H₂O, NBu₄.HSO₄, H₂O, RT, 0.5h, quantitative. f) Triphosgene, DMF, CH₂Cl₂, RT, 0.5h then 2-methoxybenzylamine, DBU, 0°C to RT, 20h, 38%. g) TFA, CH₂Cl₂, RT, 24h, 36%. h) propargylamine or homopropargylamine, pyridine, 120°C, 24h, **16**: 73% and **17**: 80%. i) **15**, pyridine, 90°C, 20h, 29%. j) CuSO₄.5H₂O, sodium ascorbate, tBuOH : H₂O (1/1), 25°C, **19**: 43% and **20**: 69%.

2.2 Biological activity and SAR studies

In vitro parasite growth inhibition assays were performed on the *P. falciparum* chloroquine-resistant FcB1 (Columbia) strain. Single point (20 μM) percentage inhibition studies were first carried out for all compounds, followed by the determination of EC₅₀ values using a 10-point dose-response assay, for the most interesting compounds (a cut-off value of > 60 % was chosen). Both experiments were run in duplicate.

Initial evaluation. In general, increasing chain length of the linker in zone B led to a loss in potency (Table 2). For instance, compound **8a** showed a 42-fold loss in inhibitory activity compared to the referent compound **7a**. Switching from the pendant 2-methoxybenzylamine **7a** to either the methoxyphenethylamine **7b** or the *o*-anisidine **7c** was not tolerated and led to a significant drop in potency. The replacement of the aromatic group with an aliphatic moiety such as isopentyl **7d** or cyclopentyl **7e** resulted in substantially inactive compounds. It is noteworthy that analogues with n = 0 are part of another cluster (MMV665878 series), which will not be discussed in this manuscript since this series might exhibit a different mode of action.

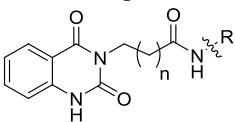
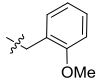
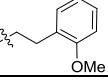
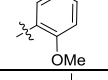
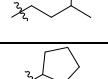
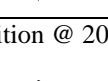
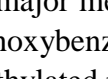
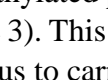
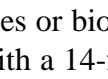
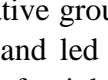
Cmpd 	n	R	EC ₅₀ FcB1 μM (% inh) ^a
MMV665916, 7a	1		0.4 ± 0.1
8a	2		16.9 ± 5.8
7b	1		10.1 ± 7.2
8b	2		7.7 ± 2.6
7c	1		(53.1 ± 1.0)
7d	1		> 25
8d	2		>25
7e	1		(32.9 ± 3.4)
8e	2		(21.3 ± 3.2)

Table 2. Initial hit expansion. ^a % inhibition @ 20 μM (in duplicate)

Modification of the *N*-benzylamide moiety. The major metabolic pathway of compound **7a** is predicted to be the *O*-demethylation of the 2-methoxybenzylamide moiety (Figure 1a, major site of metabolism highlighted in red). The *O*-demethylated putative metabolite, compound **7f**, was synthesized and was found to be inactive (Table 3). This potential metabolic instability and poor activity of its probable metabolite encouraged us to carry on further efforts to replace this methoxy moiety with metabolically stable derivatives or bioisosteres.^{20,25} Extending the chain length from methyl to ethyl **7g** was not tolerated with a 14-fold loss in potency. Replacement of this point of metabolic vulnerability with alternative groups such as -OCHF₂ **7h**, -OCF₃ **7i** or by a chlorine substituent **7j** was not tolerated and led to a significant drop in potency, suggesting that the OMe substituent is primordial for inhibitory activity. To minimize the oxidative metabolism of the aromatic anisole core, modulation of its electron density was also investigated. Fluorination on the aromatic ring, such as fluoroanisole **7k** or difluoroanisole **7l** was detrimental to activity (12-fold and 28-fold loss in potency, respectively). Moreover, the 3,5-dimethoxy arrangement **7m** was inactive.

In addition, the benzylic proton is also predicted to be vulnerable to metabolic hydroxylation, whereas the amide bond should be susceptible to hydrolytic enzymes. To mitigate these metabolic hot spots, the steric bulk around both positions was increased by either capping the free NH with the *N*-methyl amide **7n** or restricting the conformation of **7o**. These modifications resulted in a significant drop in potency and suggested NH is important for binding. Replacing the anisole core with benzimidazole **7p** or methylpyrazole **7q** were also examined, but this scaffold hopping approach was inefficient.

The substrate scope of the *N*-benzylamide part seems to be restricted to the 2-methoxybenzylamide moiety.

Cmpd	NR ¹ R ²	EC ₅₀ FcB1 μM (%inh) ^a
MMV665916, 7a		0.4 ± 0.1
7f		(17.1 ± 6.6)
7g		5.5 ± 0.7 (84.7 ± 4.6)
7h		32.0 ± 22.6 (63.8 ± 3.6)
7i		6.8 ± 2.5 (72.5 ± 4.1)
7j		37.5 ± 4.9 (56.0 ± 1.8)
7k		5.0 ± 1.41 (74.8 ± 2.7)
7l		11.3 ± 3.9 (68.3 ± 1.5)
7m		(28.0 ± 2.4)
7n		(41.8 ± 6.8)
7o		(30.6 ± 2.8)
7p		(38.1 ± 0.3)
7q		(19.9 ± 1.8)

Table 3. SAR exploration of the N-benzylamide part. ^a % inhibition @ 20 μM

Modification of the quinazolinone core. To overcome metabolic liabilities predicted at the C6 and C7 position of the quinazolinone core (Figure 1a), electron-withdrawing substituents like bromine or fluorine atom were introduced in **7r-t** compounds to block these metabolic soft spots and to reduce the electron density of the aromatic core. The addition of fluoro substituent to the 6-position **7r** or 6 and 7-positions **7s** on the aromatic portion of the quinazolinone core gave disappointing results, with the inhibitory data showing EC₅₀ values in the medium micromolar range (Table 4). The 6-bromo analogue **7t** followed a similar trend with a loss in potency, suggesting a rather shallow binding pocket around the aromatic quinazolinone core. Alternatively, as a way to mitigate oxidative metabolism,²⁶ nitrogen heteroatom was incorporated into the phenyl ring giving the azaquinazolinone derivative **7v**, which led to a drop in inhibitory activity. Substituents in the aromatic portion were not pursued further.

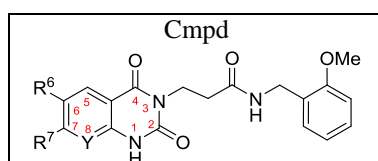
Cmpd	R ⁶	R ⁷	Y	EC ₅₀ FcB1 μM (% inh) ^a
	H	H	CH	0.4 ± 0.1
7a	H	H	CH	0.4 ± 0.1
7r	F	H	CH	20 ± 18.4 (65.4 ± 6.3)
7s	F	F	CH	(40.5 ± 1.2)
7t	Br	H	CH	(59.8 ± 0.7)
7u	H	H	N	(52.4 ± 1.8)

Table 4. SAR exploration of the quinazolinone core. The quinazolinone skeleton is numbered in red. ^a % inhibition @ 20 μM

Peptide bond isosters. The replacement of the scissile peptide bond of MMV665916 with non-hydrolyzable isosteric sulfonamide **18** and triazole **19** did not yield an effective surrogate of the parent amide system (Table 5). However, the 1,4-disubstituted triazole surrogate **20** seemed to be the best isostere. Substitution at position-1 of the triazole should be more extensively studied, but the project was halted due to a rather flat SAR study.

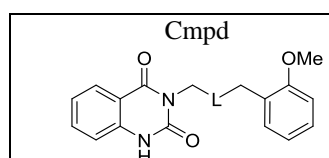
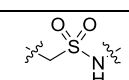
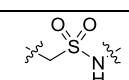
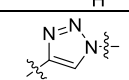
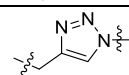
Cmpd	L	Inhibition % @ 20 μM
		21.7±5.5
18		21.7±5.5
19		30.5±2.3
20		68.85±4.05

Table 5. SAR exploration of amide bioisosteres. Mean values from a minimum of two experiments

Pharmacomodulation of the different parts of the MMV665916 compound resulted in a marked decrease of the inhibitory activity. This rather disappointing SAR studies might highlight some lack of cellular penetration or poor aqueous solubility. It also questions the potential mode of action of this series.

Possible mode of action and molecular docking. Towards the end of this project, by analyzing the *P. falciparum* resistome and druggable genome, Cowell et al.²⁷ has suggested a potential mode of action for MMV019066 (and by analogy for MMV665916) through the inhibition of the zinc-dependent farnesyltransferase PfFT enzyme (PF3D7_1147500). The protein farnesyltransferase catalyzes the transfer of a farnesyl group from a farnesyl pyrophosphate donor (FPP) to a cysteine residue within the tetrapeptide recognition sequence Ca₁a₂X (a = two small aliphatic amino acids, X is often Ser, Met, Ala, or Gln) located at the carboxyl terminus of a substrate protein,²⁸ especially small GTP-binding proteins part of the Ras superfamily (Ras, Rac, Rho and Rab). These proteins regulate many cellular processes such as cell signal transduction, vesicle trafficking and cell cycle progression.²⁹ However, their activation and function are dependent on farnesylation. Moreover, Ras mutations in human have been described in malignant transformation, invasion, and spread of cancer and are associated with 25-30% of all human cancers.³⁰

For these reason, inhibitors of protein farnesyltransferase have been developed as anticancer chemotherapeutic agents since the early 1990s and have been the focus of intense research in numerous pharmaceutical companies.^{31–35} Later on, these farnesyltransferase inhibitors were found to be highly efficacious in the treatment of pathogenic protozoa such as *Trypanosoma brucei* and *Plasmodium falciparum* and the protein farnesyltransferase has emerged as a significant target for the development of novel generation of antimalarial agents.^{36–40}

In the absence of a crystal structure of *P. falciparum* farnesyltransferase (PfFT), only a homology model can be used through comparison with its mammalian orthologs. Indeed, numerous mammalian FT – inhibitor co-crytsal structures are reported in the literature and almost all inhibitors bind to the Ca₁a₂X portion of the active site that is normally occupied by the protein substrate. As a result, FT and the inhibitor form a quaternary complex with FPP and the zinc ion. Only one ethylenediamine-scaffold-based inhibitor leads to a ternary complex by occupying both the FPP pocket and the Ca₁a₂X subsite and thereby preventing the binding of both substrates.⁴¹

In their mode of action study, Cowell et al.²⁷ proposed a potential binding mode for MMV019006 when docked to a homology model of the metalloenzyme PfFT. Surprisingly, the ligand would compete with the substrate FPP for the same hydrophobic space according to this model. Neither FPP nor the zinc (II) ion were present in the docking process. It has been shown, however, that FPP is required for the efficient binding of the ligand.⁴² Instead of a competing binding mode, we propose here a cooperative binding mode that is achieved by docking MMV019006 or MMV665916 to a homology model of PfFT in the presence of FPP and the metal ion (Figure 2a). The most favorable binding mode for both ligands is very similar. One of the carbonyl groups of the heterocycle is complexed to the metal ion. In the case of MMV019006 the sulfur of the thienopyrimidine core is complexed to the metal ion, too. For both ligands, the hydrophobic parts of the aromatic moieties interact with the hydrophobic tail of FPP providing a potential explanation for the observed cooperativity. The methoxy-substituted aromatic ring performs a parallel-displaced Pi-Pi stacking with Trp452 (4.3 Å) of the enzyme. This interaction seems to be crucial since its disruption is likely to cause emergence of resistant clones to this pyrimidinedione series. Indeed, the A515V or A515T mutations led to a 57 to 80-fold loss in potency.²⁷ Molecular dynamic simulations (Figure 2b) show that the mutation A515V displaces Trp452 inward the CaaX binding site inducing a contraction of the active site and most likely perturbing the Pi stacking with the anisole moiety of both MMV compounds.

When three analogs of MMV665916 with the lowest EC₅₀ values (**7g**, **7i**, **7k**) are docked to the ternary complex PfFT:Zn(II):FPP we observe similar binding modes as for MMV665916 (Figure 2c). All compounds display very similar ADVina docking scores (between -7.7 and -8.4 kcal/mol). The scores do not correlate with the EC₅₀ values which is not a priori surprising. First, EC₅₀ reflects only partially the energetics of binding. Second, given the complex metallo-environment of the binding site, more advanced free-energy calculations[doi.org/10.1038/s41598-020-80769-1] (with explicit water treatment and proper zinc parameters[DOI: 10.1002/prot.340230104]) would be necessary to obtain a better description of the energetics of binding.

Human farnesyltransferase has emerged as a potential therapeutic target against cancer in recent years[doi.org/10.1016/j.semcancer.2017.10.010]. When overlaying our model of PfFT with the crystal structure of human FT (PDB entry 1JCQ) we see that the active sites almost perfectly overlap (Figure 2d) and almost all residues in this site are conserved. The exception is Tyr361 (hFT) which overlays with Cys393 (PfFT). Cys393 forms the cavity for MMV665916 whereas Tyr361 interacts with Trp303 and thereby completely blocks this cavity. As a result the docking poses for MMV665916 and its analogs are very different when probed for interaction with hFT (data not shown). This indicates a different binding mode for hFT and PfFT and could potentially give rise to selectivity. Again, more experiments & sophisticated calculations would be required to address selectivity issues.

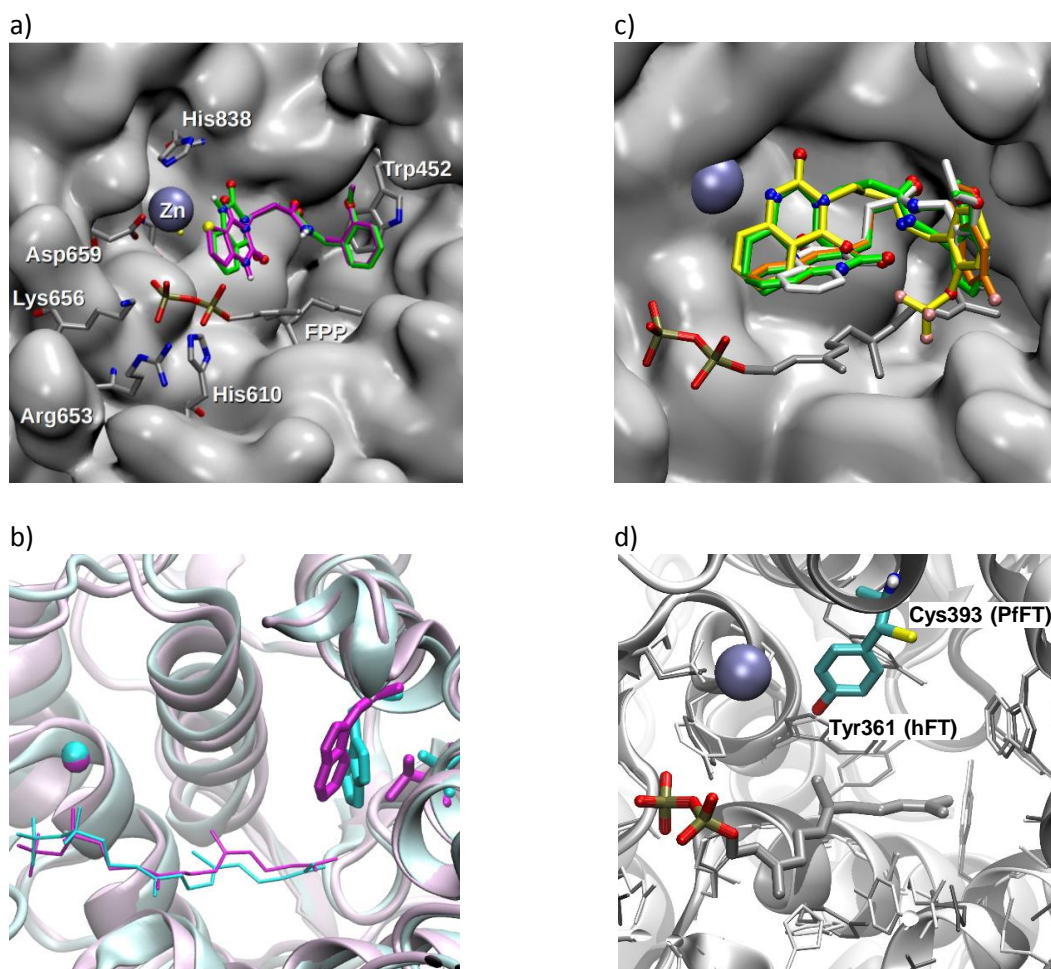


Figure 2. a) Binding mode of ligands MMV019006 (magenta) and MMV665916 (green) when docked to a model of PfFT (shown as white surface) in complex with a zinc (II) ion and FPP. Protein residues involved in the binding of the diphosphate of FPP and the metal ion are shown as thin sticks, as well as Trp452 that forms a pi-stacking interaction with the ligand. Hydrogen atoms are omitted; only polar hydrogens of the ligands are shown. b) Displacement of Trp452 due to the mutation A515V. The figure shows a time-averaged structure of the protein (cartoon model), metal ion (sphere), FPP (thin sticks) and residues 452 and 515 (thick sticks) in cyan (WT) or magenta (A515V). The time average was formed with 50 snapshots sampled during the last 50 ns of a 100 ns-long molecular dynamics simulation. c) The top-ranked pose for **7g** (white, score: -7.7 kcal/mol), **7i** (yellow, -8.4) and **7k** (orange, -8.0) when docked to the ternary complex PfFT:Zn(II):FPP. In addition the two top-ranked poses of MMV665916 (green, both with a score of -7.8) are shown. The analogs align with the best pose of MMV665916 (**7i**) or with the second-best pose (**7g**, **7k**). d) Overlay of hFT (white) and the model of PfFT (silver). Residues in the active site are shown as thin sticks. Residue Tyr361 (hFT) and Cys393 (PfFT) and FPP are shown as colored, thick sticks.

3 Conclusion

We report herein the readily preparation of twenty-seven pyrimidinedione derivatives of MMV665916. These compounds were found to display antiplasmodial activity against the erythrocytic stages of the chloroquine resistant FcB1 *Plasmodium falciparum* strain in the low to medium micromolar concentration. Our best analogues, the ethoxy derivative **7g**, the tifluoromethoxy **7i** and the fluoro analogue **7k** demonstrated the highest inhibitory activity with EC₅₀ values around 5 μM. However, we did not manage to optimize this MMV665916 series and the SAR study led to a marked decrease of the inhibitory activity compared to the reference EC₅₀ value of 0.4 μM. We also investigated the molecular docking of this pyrimidinedione series with its potential protein target, the farnesyltransferase PfFT enzyme and suggested a novel cooperative binding mode including FPP and the zinc ion. To improve the SAR study, it might be beneficial to base future modifications of MMV665916 on this new structural model of the docked ligand (that became available only towards the end of this project).

Declaration of interests

The authors declare no conflict of interest.

Acknowledgements

This work was supported by the University of Haute Alsace and the Fondation partenariale Haute Alsace. We also wish to thank the different undergraduate students involved in this project (Thomas Pancaldi, Valentin Morel, Pinar Yildirim and Rozerin Demirtas).

Supplementary data

Synthetic details and characterization for all compounds can be found in Supplementary data. All the final compounds reported herein were fully characterized by NMR spectra and HRMS. Their purity was determined to be greater than 95% by HPLC.

References

1. World Health Organization. *World Malaria Report 2020: 20 Years of Global Progress and Challenges.*; 2020:299.
2. *Artemisinin Resistance and Artemisinin-Based Combination Therapy Efficacy (December 2019).* WHO; 2019:6.
3. WHO. Malaria Threat Map. Accessed July 15, 2020. <https://apps.who.int/malaria/maps/threats/>

4. Wells TNC, Burrows JN, Baird JK. Targeting the hypnozoite reservoir of *Plasmodium vivax*: the hidden obstacle to malaria elimination. *Trends Parasitol.* 2010;26(3):145-151. doi:10.1016/j.pt.2009.12.005
5. Mazier D, Rénia L, Snounou G. A pre-emptive strike against malaria's stealthy hepatic forms. *Nat Rev Drug Discov.* 2009;8(11):854-864. doi:10.1038/nrd2960
6. Prudêncio M, Rodriguez A, Mota MM. The silent path to thousands of merozoites: the *Plasmodium* liver stage. *Nat Rev Microbiol.* 2006;4(11):849-856. doi:10.1038/nrmicro1529
7. Spangenberg T, Burrows JN, Kowalczyk P, McDonald S, Wells TNC, Willis P. The Open Access Malaria Box: A Drug Discovery Catalyst for Neglected Diseases. *PLOS ONE.* 2013;8(6):e62906. doi:10.1371/journal.pone.0062906
8. Swann J, Corey V, Scherer CA, et al. High-Throughput Luciferase-Based Assay for the Discovery of Therapeutics That Prevent Malaria. *ACS Infect Dis.* 2016;2(4):281-293. doi:10.1021/acsinfecdis.5b00143
9. Voorhis WCV, Adams JH, Adelfio R, et al. Open Source Drug Discovery with the Malaria Box Compound Collection for Neglected Diseases and Beyond. *PLOS Pathog.* 2016;12(7):e1005763. doi:10.1371/journal.ppat.1005763
10. Obach RS, Baxter JG, Liston TE, et al. The Prediction of Human Pharmacokinetic Parameters from Preclinical and In Vitro Metabolism Data. *J Pharmacol Exp Ther.* 1997;283(1):46-58.
11. Lucantoni L, Duffy S, Adjalley SH, Fidock DA, Avery VM. Identification of MMV Malaria Box Inhibitors of *Plasmodium falciparum* Early-Stage Gametocytes Using a Luciferase-Based High-Throughput Assay. *Antimicrob Agents Chemother.* 2013;57(12):6050-6062. doi:10.1128/AAC.00870-13
12. Lucantoni L, Avery V. Whole-cell in vitro screening for gametocytocidal compounds. *Future Med Chem.* 2012;4(18):2337-2360. doi:10.4155/fmc.12.188
13. Lucantoni L, Fidock DA, Avery VM. Luciferase-Based, High-Throughput Assay for Screening and Profiling Transmission-Blocking Compounds against *Plasmodium falciparum* Gametocytes. *Antimicrob Agents Chemother.* 2016;60(4):2097-2107. doi:10.1128/AAC.01949-15
14. Duffy S, Avery VM. Identification of inhibitors of *Plasmodium falciparum* gametocyte development. *Malar J.* 2013;12(1):408. doi:10.1186/1475-2875-12-408
15. Plouffe DM, Wree M, Du AY, et al. High-Throughput Assay and Discovery of Small Molecules that Interrupt Malaria Transmission. *Cell Host Microbe.* 2016;19(1):114-126. doi:10.1016/j.chom.2015.12.001
16. Ruecker A, Mathias DK, Straschil U, et al. A Male and Female Gametocyte Functional Viability Assay To Identify Biologically Relevant Malaria Transmission-Blocking Drugs. *Antimicrob Agents Chemother.* 2014;58(12):7292-7302. doi:10.1128/AAC.03666-14
17. Zaretski J, Matlock M, Swamidass SJ. XenoSite: Accurately Predicting CYP-Mediated Sites of Metabolism with Neural Networks. *J Chem Inf Model.* 2013;53(12):3373-3383. doi:10.1021/ci400518g
18. Rydberg P, Gloriam DE, Zaretski J, Breneman C, Olsen L. SMARTCyp: A 2D Method for Prediction of Cytochrome P450-Mediated Drug Metabolism. *ACS Med Chem Lett.* 2010;1(3):96-100. doi:10.1021/ml100016x

19. XenoSite Metabolism and Reactivity Prediction Web Server. XenoSite. Accessed November 27, 2017. <http://swami.wustl.edu/xenosite>
20. Meanwell NA. Synopsis of Some Recent Tactical Application of Bioisosteres in Drug Design. *J Med Chem*. 2011;54(8):2529-2591. doi:10.1021/jm1013693
21. Bachl J, Mayr J, Sayago FJ, Cativiela C, Díaz DD. Amide–triazole isosteric substitution for tuning self-assembly and incorporating new functions into soft supramolecular materials. *Chem Commun*. 2015;51(25):5294-5297. doi:10.1039/C4CC08593K
22. Gennari C, Gude M, Potenza D, Piarulli U. Hydrogen-Bonding Donor/Acceptor Scales in β -Sulfonamidepeptides. *Chem – Eur J*. 1998;4(10):1924-1931. doi:10.1002/(SICI)1521-3765(19981002)4:10<1924::AID-CHEM1924>3.0.CO;2-P
23. Sati GC, Crich D. Facile Synthesis of 3- *N* -Alkyl Pyrimidin-2,4-diones from *N* -Sulfonyloxy Maleimides and Amines. *Org Lett*. 2015;17(16):4122-4124. doi:10.1021/acs.orglett.5b02079
24. Rao YJ, Srinivas A. Synthesis of New Hybrid Heterocyclic Compounds Having 1,2,3-Triazole and Isoxazole via Click Chemistry. *J Heterocycl Chem*. 2014;51(6):1675-1678. doi:10.1002/jhet.1798
25. Meanwell NA. Fluorine and Fluorinated Motifs in the Design and Application of Bioisosteres for Drug Design. *J Med Chem*. Published online February 5, 2018. doi:10.1021/acs.jmedchem.7b01788
26. Lazzara PR, Moore TW. Scaffold-hopping as a strategy to address metabolic liabilities of aromatic compounds. *RSC Med Chem*. 2020;11(1):18-29. doi:10.1039/C9MD00396G
27. Cowell AN, Istvan ES, Lukens AK, et al. Mapping the malaria parasite druggable genome by using in vitro evolution and chemogenomics. *Science*. 2018;359(6372):191-199. doi:10.1126/science.aan4472
28. Sinensky M. Recent advances in the study of prenylated proteins. *Biochim Biophys Acta BBA - Mol Cell Biol Lipids*. 2000;1484(2):93-106. doi:10.1016/S1388-1981(00)00009-3
29. Tamanoi F, Kato- Stankiewicz J, Jiang C, Machado I, Thapar N. Farnesylated proteins and cell cycle progression. *J Cell Biochem*. 2001;84(S37):64-70. doi:10.1002/jcb.10067
30. Barbacid M. ras GENES. *Annu Rev Biochem*. 1987;56(1):779-827. doi:10.1146/annurev.bi.56.070187.004023
31. Cox AD. Farnesyltransferase Inhibitors as Anticancer Agents. In: Rak J, ed. *Oncogene-Directed Therapies*. Cancer Drug Discovery and Development. Humana Press; 2003:353-362. doi:10.1007/978-1-59259-313-2_17
32. Haluska P, Dy GK, Adjei AA. Farnesyl transferase inhibitors as anticancer agents. *Eur J Cancer*. 2002;38(13):1685-1700. doi:10.1016/S0959-8049(02)00166-1
33. Sebti SM, Hamilton AD. Farnesyltransferase and geranylgeranyltransferase I inhibitors and cancer therapy: Lessons from mechanism and bench-to bedside translational studies. *Oncogene*. 2000;19(56):6584-6593. doi:10.1038/sj.onc.1204146
34. Appels NMGM, Beijnen JH, Schellens JHM. Development of Farnesyl Transferase Inhibitors: A Review. *The Oncologist*. 2005;10(8):565-578. doi:10.1634/theoncologist.10-8-565
35. Moorthy NSHN, Sousa SF, Fernandes MJR and PA. Farnesyltransferase Inhibitors: A Comprehensive Review Based on Quantitative Structural Analysis. *Current Medicinal Chemistry*.

36. Eastman RT, Buckner FS, Yokoyama K, Gelb MH, Voorhis WCV. Thematic review series: Lipid Posttranslational Modifications. Fighting parasitic disease by blocking protein farnesylation. *J Lipid Res.* 2006;47(2):233-240. doi:10.1194/jlr.R500016-JLR200
37. Glenn MP, Chang S-Y, Hucke O, et al. Structurally Simple Farnesyltransferase Inhibitors Arrest the Growth of Malaria Parasites. *Angew Chem Int Ed.* 2005;44(31):4903-4906. doi:10.1002/anie.200500674
38. Glenn MP, Chang S-Y, Hornéy C, et al. Structurally Simple, Potent, Plasmodium Selective Farnesyltransferase Inhibitors That Arrest the Growth of Malaria Parasites. *J Med Chem.* 2006;49(19):5710-5727. doi:10.1021/jm060081v
39. Nallan L, Bauer KD, Bendale P, et al. Protein Farnesyltransferase Inhibitors Exhibit Potent Antimalarial Activity. *J Med Chem.* 2005;48(11):3704-3713. doi:10.1021/jm0491039
40. Fletcher S, Cummings CG, Rivas K, et al. Potent, Plasmodium-Selective Farnesyltransferase Inhibitors That Arrest the Growth of Malaria Parasites: Structure–Activity Relationships of Ethylenediamine-Analogue Scaffolds and Homology Model Validation. *J Med Chem.* 2008;51(17):5176-5197. doi:10.1021/jm800113p
41. Hast MA, Fletcher S, Cummings CG, et al. Structural Basis for Binding and Selectivity of Antimalarial and Anticancer Ethylenediamine Inhibitors to Protein Farnesyltransferase. *Chem Biol.* 2009;16(2):181-192. doi:10.1016/j.chembiol.2009.01.014
42. Reid TS, Beese LS. Crystal Structures of the Anticancer Clinical Candidates R115777 (Tipifarnib) and BMS-214662 Complexed with Protein Farnesyltransferase Suggest a Mechanism of FTI Selectivity. *Biochemistry.* 2004;43(22):6877-6884. doi:10.1021/bi049723b